Catalysis |*Hot Paper*|

Urea-Substituted Tetramethylcyclopentadienyl Ligands for Supramolecularly Accelerated Rh^{III}-Catalyzed *ortho*-C–H Olefination of Benzoic Acid Derivatives

David Maurer and Bernhard Breit*[a]

Abstract: The design and synthesis of air-stable and conveniently crystallizable Rh^{III}-cyclopentadienyl catalysts substituted with a urea moiety, which are able to accelerate the C–H olefination of benzoic acid derivatives, is reported. Through kinetic studies and NMR titration experiments, the catalysts' substrate recognition ability mediated by hydrogen bonding was identified to be the reason for this effect. Introduction of pyridone-phosphine ligands capable of forming additional H-bond interactions increased the catalytic performance even further. By unveiling a proportionality between reaction rate and relative complex formation enthalpy the hypothesis of a supramolecular catalyst preformation was supported. Its application to a variety of substrates proved the catalyst system's advantages, generally increasing the yields when compared to the results obtained with widely used $[RhCp^*Cl_2]_2$.

Nature provides a sheer endless number of examples of catalytic reactions accelerated by enzymes able to recognize their respective substrates with the help of non-covalent interactions such as hydrogen bonds, electrostatic interactions, or π-stacking.[1,2] Inspired chemists have been able to benefit from this toolbox by designing artificial enzymes featuring biomimetic catalytic properties for several decades.[3,4] Recent publications have successfully demonstrated that similar concepts can also be applied to transition metal-catalyzed C–H activation: bipyridine ligands designed for iridium-catalyzed C–H borylation of aromatic substrates have been studied intensively and have provided access to regioselective *meta*-,[5,6] *para*-,[7] and *ortho*-functionalization[8] (Figure 1 a). Our own group's efforts to develop supramolecular catalyst systems have been focused on reactions catalyzed by rhodium. Early examples include a library of monodentate phosphine ligands functioning as bidentate ligands through self-assembly via hydrogen bonding[9] or a regioselective hydroformylation of α,β-unsaturated carboxylic acids, which was achieved using phosphine ligands bearing an acyl-guanidine moiety as the substrate recognition group.[10] Intrigued by the results obtained using side chain-functionalized cyclopentadienyl rhodium catalysts (examples: Figure 1 b)

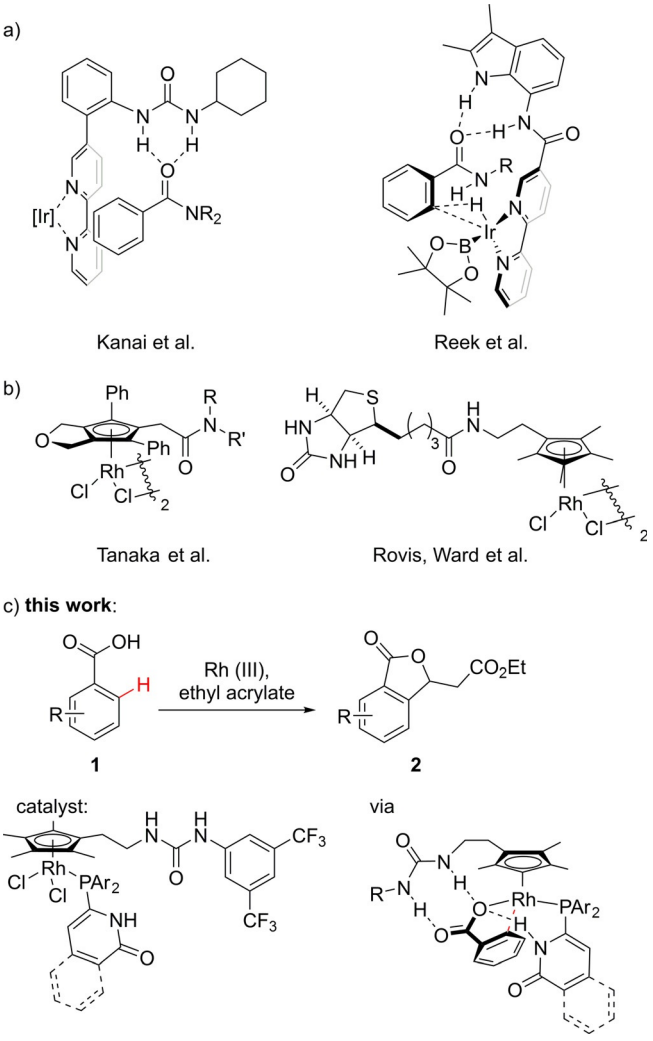

Figure 1. a) Examples of previous work on Ir-catalyzed C–H borylation involving H-bond interactions. b) Selection of previous examples of functionalized RhCp* catalysts. c) Rh-catalyzed C–H activation accelerated by H-bond interactions between substrate and catalyst system.

[a] *D. Maurer, Prof. Dr. B. Breit*
Institut für Organische Chemie, Albert-Ludwigs-Universität Freiburg
Albertstraße 21, 79104 Freiburg (Germany)
E-mail: bernhard.breit@chemie.uni-freiburg.de

Supporting information and the ORCID identification number(s) for the author(s) of this article can be found under: https://doi.org/10.1002/chem.202005130.

in C–H functionalization chemistry,[11,12] we were eager to investigate if this class of catalysts could be derivatized to include a substrate recognition group capable of establishing a secondary interaction strong enough to have a significant effect on rhodium-catalyzed C–H activation. To the best of our knowledge, only iridium-catalyzed borylation reactions have been successfully improved through this kind of supramolecular approach so far.[13]

The synthesis of a $Rh^{III}Cp^*$-dimer bearing a pendant primary amine group being reported in ref. [14], we chose a urea residue as a conveniently accessible recognition group that would serve as a hydrogen bond-donor towards an appropriate substrate. Conceivably, the addition of a 6-DPPon [6-(diphenylphosphaneyl)pyridin-2(1*H*)-one] ligand derivative to the resulting catalyst dimers would not only result in a significantly greater catalyst variability, but also introduce an additional flexible H-bond donor/acceptor system due to its versatile 2-pyridone residue.

In order to evaluate our catalysts' performance, we chose the well-established Rh^{III}-catalyzed C–H olefination of benzoic acid derivatives **1** as our benchmark reaction, leading to lactones **2** via subsequent Michael addition.[15–20] Hypothetically, a supramolecular preorganization between catalyst and substrate might lead to an intermediate stabilized by hydrogen bonds between the carboxylic acid and both the urea- and the 2-pyridone moiety (Figure 1c).

In an initial unpublished study, we had identified Rh^{III}-dimer **3** bearing a 3,5-bis(trifluoromethyl)phenyl residue as a potent catalyst for the *ortho*-C–H olefination of 1-naphthoic acid (for condition screening: see Supporting Information, Tables S5–S7). Catalyst derivatives bearing diverse other alkyl- or aryl-substituents at the urea moiety had proven to be less efficient in this transformation. We therefore decided to lead our investigation on the effects of 6-DPPon ligand derivatives starting from compound **3**. Introduction of all shown phosphine ligands led to air and temperature stable Rh^{III}-monomers (Figure 2), which could be conveniently purified by recrystallization and which we were able to further characterize by means of X-ray crystallography.

To our delight, crystallographic analysis of monomers **4b** and **4c** confirmed our catalyst's capability of forming intermolecular H-bonds: in crystalline solid state two monomers were found to form dimers via H-bonding between their urea-moieties and the 2-pyridone's carbonyl group (Figure 3). Furthermore, we were able to confirm dimer aggregation of complex **4b** via H-bonding interactions in solution by a ^{1}H NMR dilution experiment (see Supporting Information, Figure S5). Contrarily, no such interactions were observed in the crystal structure of 3,5-bis(trifluoromethyl)phenyl derivative **4d**, presumably for steric reasons. Methylation of the hydroxypyridine moiety's oxygen atom leading to control derivative **4e** obviously also interfered with the catalyst's ability to form intermolecular hydrogen bonds resulting in a lack of dimerization in its crystal structure (see Supporting Information for CIF-files and render images).

In order to evaluate our catalyst's performance in C–H activation, we chose to analyze the aforementioned Rh^{III}-catalyzed

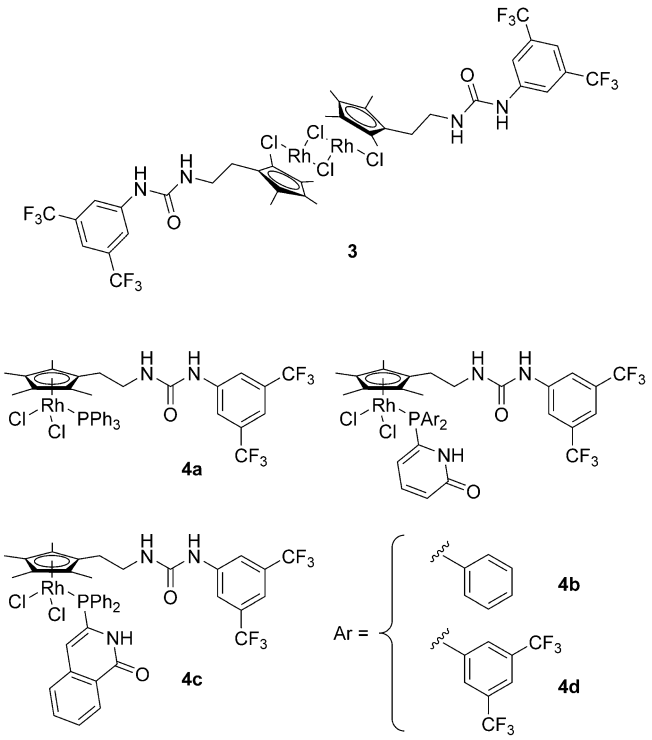

Figure 2. Overview of urea-substituted $Rh^{III}Cp^*$-catalysts presented in this work.

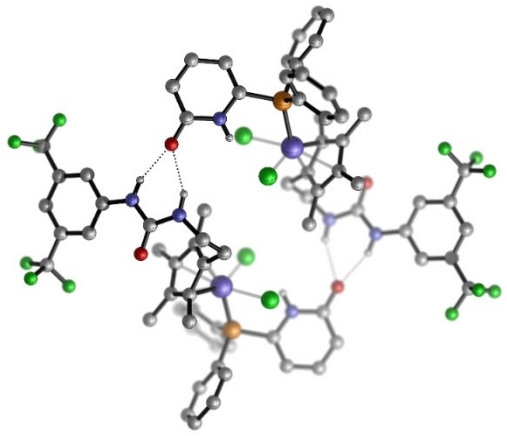

Figure 3. X-ray structure of ligand **4b** showing dimerization via H-bonding between urea and 2-pyridone moieties [*d*(NH···O) = 2.00 and 2.21 Å]. Carbon-bound H-atoms and solvent molecules were omitted for clarity.

ortho-C–H olefination kinetically. 1-Naphthoic acid **1a** was chosen as the model substrate to simplify the process because neither bis-functionalized product nor regioisomers were to be expected. The primarily formed olefin product was observed to be at nearly constant concentration over time. Expecting the subsequent Michael addition leading to lactone **2a** to be significantly faster than the initial C–H-functionalization reaction, we decided to assume the olefin's concentration to be quasi-stationary. In consideration of the constant excess of ethyl acrylate during the reaction, we chose to calculate a pseudo-first order rate constant with respect to the concentra-

tion of 1-naphthoic acid **1a** (see Supporting Information for experimental details). As a result of our experiment, we were able to observe an acceleration of about 50% when comparing catalyst dimer **3** to commercially available $[RhCp^*Cl_2]_2$. To our delight, the monomers deriving from 6-DPPon (**4b**) and 3-DPICon [3-(diphenylphosphaneyl)isoquinolin-1(2*H*)-one, **4c**] performed even more efficiently, showing an increase of the relative rate constant by a factor of 2.2 and 1.8, respectively. A variation of the phosphine ligand's aryl substituents from phenyl to 3,5-bis(trifluoromethyl)phenyl (**4d**) led to a less significant acceleration ($k_{rel}=1.3$). On the other hand, using triphenylphosphine monomer **4a** as the catalyst, a reaction rate comparable to the parent compound $[RhCp^*Cl_2]_2$ was observed (Figure 4a). We therefore hypothesized a cooperative effect including not only a non-covalent interaction between the catalyst's urea moiety and the substrate but also involving the phosphine ligand's 2-pyridone residue. Variable-temperature ^{1}H NMR experiments of catalyst **4b** in the presence of 1-naphthoic acid **1a** confirmed the presence of H-bonding interactions at the reaction temperature (see Supporting Information, Figure S6).

In an attempt to justify our assumption, we conducted several control experiments (Figure 4b). Catalyst monomer **4e**, being similar to catalyst **4b** with the exception of its hydroxypyridine moiety being *O*-methylated, performed significantly worse ($k_{rel}=1.2$) than its free 2-pyridone analogue. We therefore concluded that the 2-pyridone's nitrogen-H-bond donor functionality might play a key role in the catalyst's activity. Furthermore, we were able to rule out the possibility of the reaction simply being accelerated by the presence of a free urea or phosphine ligand: while the reaction rate was not affected by the presence of urea **5a** (10 mol%), the reaction was even slowed down when either triphenyl phosphine (10 mol%, $k_{rel}=0.4$) or 6-DPPon **5b** (10 mol%, $k_{rel}=0.8$) were used in combination with $[RhCp^*Cl_2]_2$.

In order to support our hypothesis of the reaction being accelerated by a supramolecular catalyst pre-assembly involving the substrate's carboxylic acid function as well as the catalyst's urea and presumably 2-pyridone moieties, we performed a series of ^{1}H NMR titration experiments.[21] An increase of substrate (1-naphthoic acid **1a**) concentration relative to a constant concentration of each given catalyst resulted in a significant downfield shift of the respective urea residue's nitrogen-bound proton signals (Figure 5a). The data thereby obtained was analyzed using the platform http://supramolecular.org provided by Hibbert and Thordarson (see Supporting Informa-

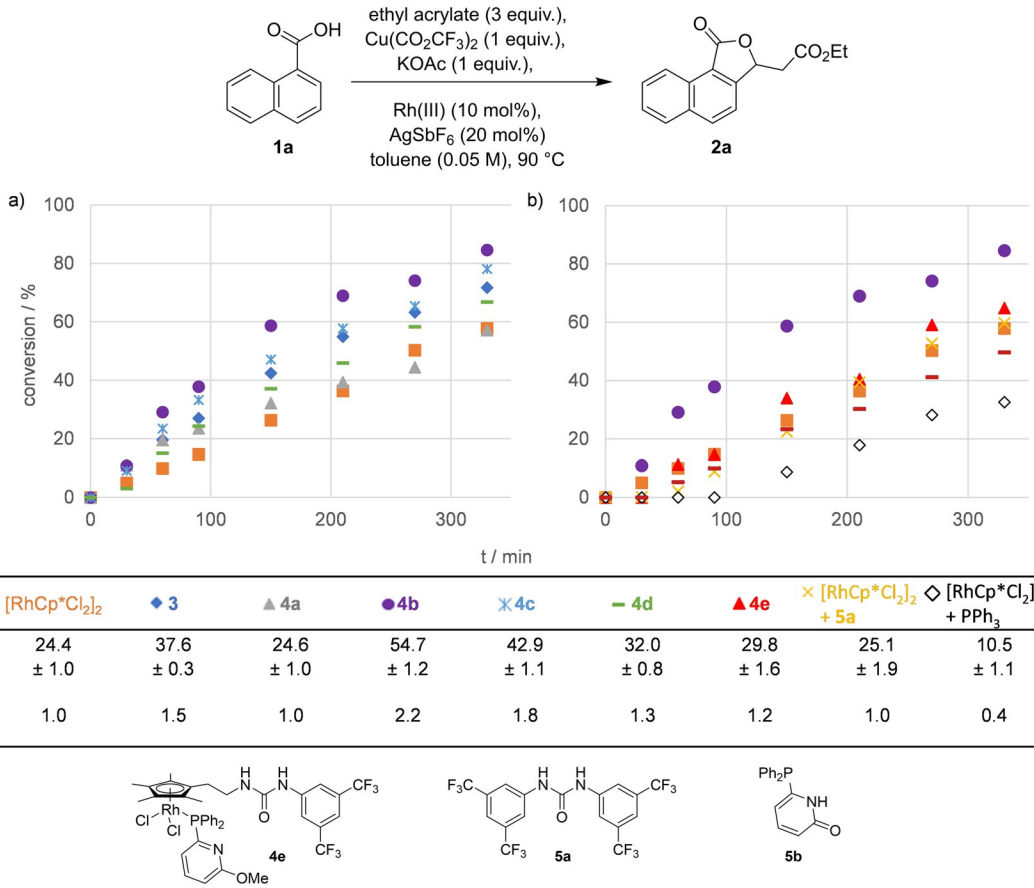

c)

catalyst	■ $[RhCp^*Cl_2]_2$	◆ 3	▲ 4a	● 4b	✳ 4c	– 4d	▲ 4e	× $[RhCp^*Cl_2]_2$ + 5a	◇ $[RhCp^*Cl_2]_2$ + PPh_3	– $[RhCp^*Cl_2]_2$ + 5b
k / 10^{-4} min^{-1}	24.4 ± 1.0	37.6 ± 0.3	24.6 ± 1.0	54.7 ± 1.2	42.9 ± 1.1	32.0 ± 0.8	29.8 ± 1.6	25.1 ± 1.9	10.5 ± 1.1	19.1 ± 0.8
k (catalyst n) / k ($[RhCp^*Cl_2]_2$)	1.0	1.5	1.0	2.2	1.8	1.3	1.2	1.0	0.4	0.8

Figure 4. a) Kinetic evaluation of the *ortho*-C–H olefination of 1-naphthoic acid **1a** catalyzed by the Rh^{III}-complexes presented in this work; graphical representation of the substrate's conversion to lactone **2a** plotted against the reaction time. b) Control experiments. c) Rate constants (k) were calculated assuming the primarily formed olefin's concentration to be quasi-stationary; rate constants (k_{rel}) relative to the parent compound $[RhCp^*Cl_2]_2$ are given for facilitated comparability.

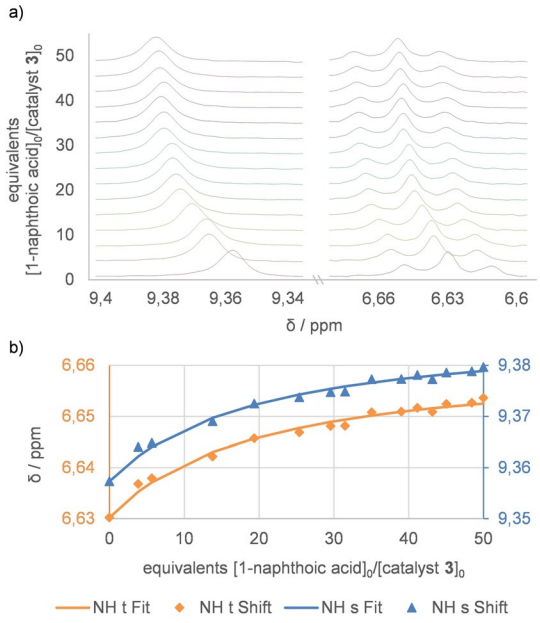

c)

catalyst	ΔG_{rel} / kJ mol^{-1}	K / M^{-1}
3	4.5 ± 0.4	20.5 ± 1.9
4a	0	3.3 ± 0.6
4b	8.4 ± 1.0	96 ± 11
4c	6.0 ± 1.0	37 ± 6
4d	2.1 ± 0.3	7.6 ± 1.0
4e	0.2 ± 0.1	3.5 ± 0.3

Figure 5. a) ^{1}H NMR shifts of catalyst **3's** urea NH-signals relative to the equivalents of 1-naphthoic acid (**1a**, substrate) added via titration. b) ^{1}H NMR data (urea NH-signals) obtained from titration of catalyst **3** with 1-naphthoic acid **1a** fitted for a guest/host stoichiometry of 1:1. c) Relative Gibbs energies of complex formation (ΔG_{rel}) and average complex association constants (K) between each catalyst and 1-naphthoic acid **1a** resulting from NMR titration experiments.

tion for further details).[22] Figure 5 illustrates this process on the example of a solution of catalyst dimer **3** (0.0025 M) to which increasing amounts of 1-naphthoic acid (0 to 50 equiv.) were added. The experimentally obtained NMR shifts (triplet: orange diamonds, singlet: blue triangles, Figure 5b) were fitted assuming a 1:1 catalyst to substrate ratio for the newly formed complex, thereby giving access to an association constant. Similar experiments were conducted at least twice for each catalyst shown in Figure 2. Relative Gibbs energies of complex formation were calculated from the resulting average binding constants defining the lowest value obtained for triphenyl phosphine derivative **4a** as a reference. (Figure 5c, details in Supporting Information, Tables S3–S4). The highest value of 8.4 kJ mol^{-1} was obtained for catalyst **4b**, whereas significantly lower relative free binding energies were found for its *O*-methylated analogue **4e** (0.2 kJ mol^{-1}). These findings seem to indicate that the presence of a 6-DPPon ligand derivative effectively strengthens the substrate recognition via the catalysts' urea moieties, thereby further supporting our hypothesis of a cooperative effect.

Intriguingly, when plotting the aforementioned relative free binding energies (Figure 5) against the rate constants resulting from our kinetic evaluations (Figure 4), an approximately linear relationship can be observed (Figure 6a). In conclusion to the observations described so far, we propose that a non-covalent stabilization of the reaction intermediates seems to be induced by H-bonding interactions involving the catalyst's urea residue and the substrate's carboxylic acid moiety. The presence of a 6-DPPon ligand derivative seems to strengthen this supramolecular assembly. This cooperative effect might lower activation barriers during the catalytic cycle, thereby accelerating the reaction rate of the studied C–H functionalization. A hypothetical intermediary *ortho*-metalated species is shown in Figure 6b, demonstrating a supramolecular mode of stabilization in agreement with our initial hypothesis: two H-bonds might be formed between the urea residue's nitrogen-bound hydrogen atoms and the carboxylic acid, while a third H-bond to the 2-pyridone's N–H group is conceivable.

Having identified Rh^{III}-species **4b** as the most potent of our catalysts, we decided to explore its activity towards a broader substrate scope. In order to demonstrate its advantages, each catalytic transformation was also performed using commercially available [RhCp*Cl$_2$]$_2$ and the dimeric derivative **3**. The model reaction of 1-naphthoic acid with several activated olefins showed a clear tendency in favor of 6-DPPon-monomer **4b**: in all examined examples, product yields increased significantly when the reaction was carried out using catalyst **4b**. While in most cases an increase of about 20–30% was observed, the yield could be doubled when using sterically more demanding *tert*-butyl acrylate as the olefin (Table 1).

Aiming to explore functional group tolerance and the effect of different substituents on the catalysts' activity, we subjected a variety of aromatic substrates to our initial reaction condi-

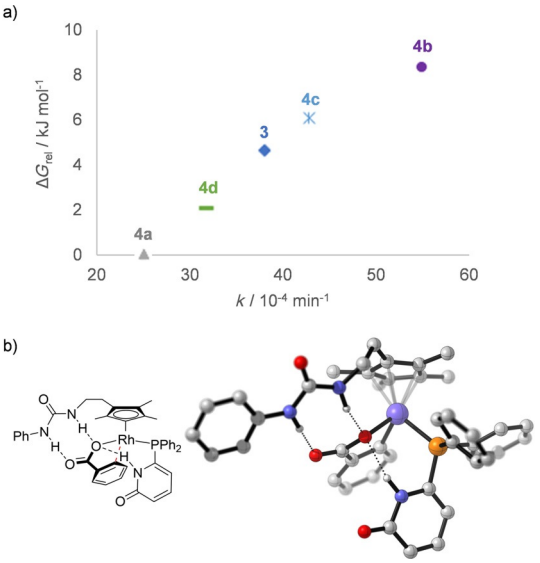

Figure 6. a) Relative Gibbs free energies (ΔG_{rel}) resulting from complex formation between catalyst and substrate plotted against the rate constants (k) obtained for *ortho*-C–H functionalization of 1-naphthoic acid **1a** catalyzed by the respective Rh^{III}-species. b) Proposed structure of *ortho*-metalated benzoic acid stabilized by H-bonding (dotted lines) to the catalyst's urea and 2-pyridone residues via its carboxylic acid function, geometrically optimized by DFT calculations (BP86/def2-SVP).

tions, comparing again the yields obtained with catalyst **4b** to those resulting from dimer **3** and $[RhCp^*Cl_2]_2$. In the case of electron-donating groups such as methyl- (**2i**) or methoxy-substituents (**2j**), *ortho*-functionalized substrates proved to be less affected by the increased performance of our catalyst systems, showing only slight yield improvements. In stark contrast, product **2h**, bearing a trifluoromethyl-group commonly found in bio-active compounds, was obtained in 65% yield with cata-

Table 1. Olefin scope of *ortho*-C–H functionalization of 1-naphthoic acid (**1a**) comparing the yields resulting from catalysts **3** and **4b** to $[RhCp^*Cl_2]_2$.[a]

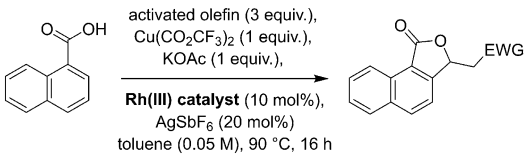

Catalyst	Yield [%]				
	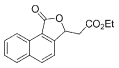	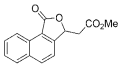	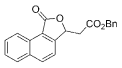	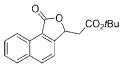	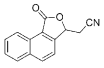
	2a	**2b**	**2c**	**2d**	**2e**
4b	91	93	83	81	50
3	85	69	73	79	47
$[RhCp^*Cl_2]_2$	69	66	68	40	39

[a] All reactions were performed at a 0.1 mmol scale. All yields were determined by ^{1}H NMR analysis of the crude reaction mixture relative to 1,3,5-trimethoxybenzene as the internal standard.

Table 2. Aryl carboxylic acid derivative scope of *ortho*-C–H functionalization with ethyl acrylate comparing the yields resulting from catalysts **3** and **4b** to $[RhCp^*Cl_2]_2$.[a]

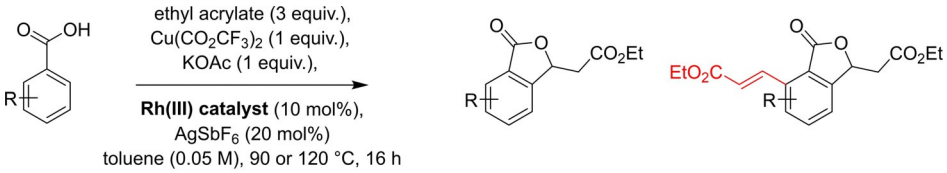

Catalyst	Yield [%]				
	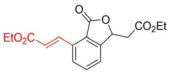	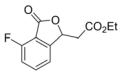	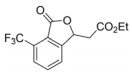	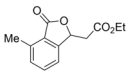	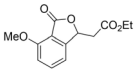
	2f	**2g**	**2h**	**2i**	**2j**
4b	47; 52[b]	78	65	89[b]	82[b]
3	41; 49[b]	77	60	86[b]	75[b]
$[RhCp^*Cl_2]_2$	36; 34[b]	75	11	84[b]	70[b]
	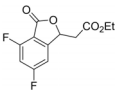	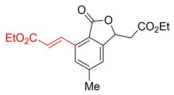	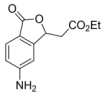	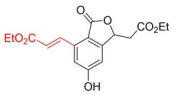	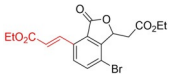
	2k	**2l**	**2m**	**2n**	**2o**
4b	70	38; 30[b]	38	54; 40	66[c]; 27
3	69	12; 39[b]	38	40; 38	63[c]; 18
$[RhCp^*Cl_2]_2$	67	13; 29[b]	30	43; 27	46[c]; 12
	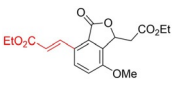	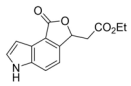	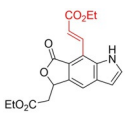	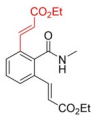	
	2p	**2q**	**2r**	**2s**	
4b	70[c]; 21[b]	30	49[c]; 24	77; 8	
3	49[c]; 30[b]	22	47[c]; 22	76; 6	
$[RhCp^*Cl_2]_2$	35[c]; 33[b]	14	20[c]; 14	59; < 5	

[a] All reactions were performed at a 0.1 mmol scale and at 120 °C if not mentioned otherwise. All yields were determined by ^{1}H NMR analysis of the crude reaction mixture relative to 1,3,5-trimethoxybenzene as the internal standard (first value: yields of mono-functionalized products; second value: yields of bis-functionalized products). [b] Reactions were performed at 90 °C. [c] Combined yield of two regioisomers.

lyst **4b** (60% with catalyst **3**), while only 11% yield were observed when using the commercially available catalyst. As for halogen atoms in *ortho*-position, only fluorine (**2g**) was tolerated under the reaction conditions; chlorine and bromine were substituted leading to products identical to those derived from unsubstituted benzoic acid (**2f**). Substituents in *para*-position were generally tolerated, resulting in mixtures of mono- and bis-functionalized products. While the yields increased only slightly for the *para*-amino (**2m**) and *para*-hydroxy (**2n**) substituted derivatives, a much more significant effect was observed for *para*-methylated product **2l**. We therefore presume that the presence of other H-bond donors than the substrate's carboxylic acid moiety obstructs the non-covalent interactions responsible for our catalyst system's advantages. Contrarily to the *ortho*-analogue, bromine was well tolerated as a substituent in *meta*-position (**2o**). Significantly higher total yields were obtained for *meta*-methoxy derivative **2p** using catalyst **4b** (91%) and **3** (79%) compared to $[RhCp^*Cl_2]_2$ (68%).

A major improvement was also observed for indole-carboxylic acid derivatives **2q** and **2r**, as Rh^{III}-monomer **4b** approximately doubled the total yields relative to the commercially available catalyst. *N*-Methylbenzamide (leading to products **2s**) proved to be a viable substrate as well, demonstrating that directing groups other than carboxylic acid interact with our catalyst system in a presumably similar fashion (Table 2).

In summary, we report that $Rh^{III}Cp^*$ complexes substituted with a urea-moiety are able to accelerate the *ortho*-C–H-olefination of carboxylic acid derivatives when compared to the widely used $[RhCp^*Cl_2]_2$. The introduction of a 6-DPPon-type ligand to the system improves the catalyst's efficiency even further, resulting in significantly increased yields for less reactive substrates. We were able to demonstrate that a non-covalent secondary interaction between the substrate's carboxylic acid function and the catalyst's urea residue is responsible for the enhanced performance, revealing a proportionality between the reaction rate and the Gibbs free energy of complex formation between substrate and catalyst. The catalyst system's applicability to other substrates and different chemical transformations is currently under investigation.

Acknowledgements

We gratefully acknowledge Lucas Baumer for his considerable assistance with laboratory experiments and Monika Lutterbeck and Günter Leonhardt-Lutterbeck for their skillful support repeating syntheses of catalysts. We thank Dr. Daniel Kratzert for X-ray crystal structure analysis, Dr. Manfred Keller for NMR analysis and Felix Bauer for DFT structure optimization. This work was supported by the DFG and the Studienstiftung des deutschen Volkes e.V. (PhD Scholarship to DM). Open access funding enabled and organized by Projekt DEAL.

Conflict of interest

The authors declare no conflict of interest.

Keywords: acceleration of catalytic reactions · C–H activation · hydrogen bonds · non-covalent substrate recognition · supramolecular chemistry

[1] J. Kraut, *Science* **1988**, *242*, 533 – 540.
[2] J. R. Knowles, *Nature* **1991**, *350*, 121 – 124.
[3] R. Breslow, *Acc. Chem. Res.* **1980**, *13*, 170 – 177.
[4] R. Breslow, *Science* **1982**, *218*, 532 – 537.
[5] Y. Kuninobu, H. Ida, M. Nishi, M. Kanai, *Nat. Chem.* **2015**, *7*, 712 – 717.
[6] H. J. Davis, M. T. Mihai, R. J. Phipps, *J. Am. Chem. Soc.* **2016**, *138*, 12759 – 12762.
[7] M. E. Hoque, R. Bisht, C. Haldar, B. Chattopadhyay, *J. Am. Chem. Soc.* **2017**, *139*, 7745 – 7748.
[8] S.-T. Bai, C. B. Bheeter, J. N. H. Reek, *Angew. Chem. Int. Ed.* **2019**, *58*, 13039 – 13043; *Angew. Chem.* **2019**, *131*, 13173 – 13177.
[9] B. Breit, *Angew. Chem. Int. Ed.* **2005**, *44*, 6816 – 6825; *Angew. Chem.* **2005**, *117*, 6976 – 6986.
[10] T. Šmejkal, B. Breit, *Angew. Chem. Int. Ed.* **2008**, *47*, 3946 – 3949; *Angew. Chem.* **2008**, *120*, 4010 – 4013.
[11] T. K. Hyster, L. Knorr, T. R. Ward, T. Rovis, *Science* **2012**, *338*, 500 – 503.
[12] S. Yoshizaki, Y. Shibata, K. Tanaka, *Angew. Chem. Int. Ed.* **2017**, *56*, 3590 – 3593; *Angew. Chem.* **2017**, *129*, 3644 – 3647.
[13] X. Lu, Y. Yoshigoe, H. Ida, M. Nishi, M. Kanai, Y. Kuninobu, *ACS Catal.* **2019**, *9*, 1705 – 1709.
[14] T. Reiner, D. Jantke, A. Raba, A. N. Marziale, J. Eppinger, *J. Organomet. Chem.* **2009**, *694*, 1934 – 1937.
[15] K. Ueura, T. Satoh, M. Miura, *Org. Lett.* **2007**, *9*, 1407 – 1409.
[16] K. Ueura, T. Satoh, M. Miura, *J. Org. Chem.* **2007**, *72*, 5362 – 5367.
[17] Q. Jiang, C. Zhu, H. Zhao, W. Su, *Chem. Asian J.* **2016**, *11*, 356 – 359.
[18] Y.-Q. Zhu, J.-X. Li, T.-F. Han, J.-L. He, K. Zhu, *Eur. J. Org. Chem.* **2017**, 806 – 811.
[19] S. W. Youn, H. J. Yoo, *Adv. Synth. Catal.* **2017**, *359*, 2176 – 2183.
[20] Y. Qiu, W. J. Kong, J. Struwe, N. Sauermann, T. Rogge, A. Scheremetjew, L. Ackermann, *Angew. Chem. Int. Ed.* **2018**, *57*, 5828 – 5832; *Angew. Chem.* **2018**, *130*, 5930 – 5934.
[21] P. Thordarson, *Chem. Soc. Rev.* **2011**, *40*, 1305 – 1323.
[22] D. Brynn Hibbert, P. Thordarson, *Chem. Commun.* **2016**, *52*, 12792 – 12805.

Manuscript received: November 27, 2020
Accepted manuscript online: December 9, 2020
Version of record online: January 18, 2021